Nanoscale

RSC Publishing

PAPER

View Article Online
View Journal | View Issue

Cite this: *Nanoscale*, 2013, **5**, 5435

Label-free electrochemiluminescent detection of DNA by hybridization with a molecular beacon to form hemin/G-quadruplex architecture for signal inhibition

Shengyuan Deng, Lingxiao Cheng, Jianping Lei, Yan Cheng, Yin Huang and Huangxian Ju*

Received 4th November 2012
Accepted 5th December 2012

DOI: 10.1039/c2nr33471b

www.rsc.org/nanoscale

A facile label-free electrochemiluminescent (ECL) DNA sensor was designed using a molecular beacon with a guanine-rich stem as a recognition probe. The ECL emission was produced from surface unpassivated CdTe quantum dots (QDs) co-immobilized with colloidal gold nanoparticles (AuNPs) on a chitosan-modified electrode surface. The molecular beacon was adsorbed onto the AuNPs by the thiolated stem. Upon the hybridization of the molecular beacon with target DNA to open the cycle in the presence of hemin, the dissociated guanine-rich sequence could conjugate hemin to form a G-quadruplex architecture. The formed DNAzyme then catalyzed the reduction of dissolved oxygen, the endogenous coreactant for ECL emission of QDs, leading to a decrease in ECL signal. The variations in surface morphology during the fabrication and recognition processes of the ECL sensor were characterized by atomic force microscopy and electrochemical impedance spectroscopy. The ECL signal inhibition depended linearly on the logarithmic value of DNA concentration ranging from 5.0 fM to 0.1 nM, with a detection limit of 0.9 fM. This proposed label-free method is a promising application of QDs-based ECL emission for ultrasensitive DNA assay.

Introduction

Due to the imperative requirements of molecular diagnosis, gene therapy and early screening for tumors, the detection of specific oligonucleotide sequences has drawn widespread attention.[1] The development of a highly sensitive strategy for the detection of DNA, especially at low physiological levels, is therefore of great importance. Various analytical technologies such as fluorescence, chemiluminescence and electrochemistry have been implemented for DNA detection.[2–5] Owing to its intrinsic sensitivity and low background, QDs-based electrochemiluminescence (ECL) technique has attracted considerable attention in DNA analysis.[6–8] For example, a method has been proposed for the ECL detection of DNA by DNA-induced separation between the excited CdS:Mn QDs and gold nanoparticles (AuNPs) to enhance surface plasmon resonance (SPR),[7] and the ECL emission from CdS QDs quenched by CdTe QDs-labeled probe DNA as black bodies has been utilized for DNA detection in a sandwich format.[8] These mechanisms afford sensitive protocols for ECL detection of DNA. However, the complicated labeling procedure and distance-dependent ECL signal transduction restrict their practical application. This work presents a facile and reliable label-free ECL method for the detection of DNA by the *in situ* formation of DNAzyme to catalyze the reduction of dissolved oxygen, the coreactant of QDs-based ECL emission.

DNAzymes as enzyme mimics have gradually achieved applications in biosensing due to their high catalytic activity and good stability.[9–12] By using DNAzyme as an electron acceptor and QD as an electron donor, a DNA detection method based on the annihilation of fluorescence (PL) emission from QDs has been constructed.[9] The hemin/G-quadruplex structure has also been implemented as a label to develop sensitive SPR sensing platforms for Pb^{2+} ions.[12] G-quadruplex-based DNAzyme can act as horseradish peroxidase (HRP) to catalyze the reduction of H_2O_2 or dissolved oxygen by some redox-active reagents or an electrocatalytic process. Thus it has been used as a label to sensitively detect DNA hybridization and proteins.[10,13,14] For example, a chemiluminescence detection method based on the catalysis of the G-quadruplex-based DNAzyme toward the oxidation of luminol by H_2O_2 has been proposed for analysis of the target adenosine and DNA in the solution.[11] This DNAzyme has also been assembled on AuNPs to label signal antibodies for immunoassay by the electrocatalytic reduction of dissolved oxygen to consume the ECL coreactant.[15]

Here, signal inhibition based on the consumption of the ECL coreactant by electrocatalytic reduction has for the first time been introduced into DNA detection by using a molecular beacon with a thiolated guanine-rich stem (MB) as a recognition probe (Scheme 1). The hairpin conformation of the MB

State Key Laboratory of Analytical Chemistry for Life Science, School of Chemistry and Chemical Engineering, Nanjing University, Nanjing 210093, P. R. China. E-mail: hxju@nju.edu.cn; Fax: +86 25-8359-3593

remained "closed" in the presence of the target only, due to the partial complementarity of the target to the long MB sequence. With the assistance of hemin, the hairpin could be dissociated upon the hybridization of MB with the target DNA. The G-quadruplex-based DNAzyme was thus formed by the binding of hemin with the guanine-rich sequence to catalyze the electroreduction of dissolved oxygen, leading to a decrease in ECL emission. The proposed label-free method for DNA detection showed a high sensitivity, wide detection range and excellent specificity, and thus possesses promise for sensing application.

Experimental

Materials and reagents

Hemin, 6-mercapto-1-hexanol (MCH), ethanolamine, *N*-hydroxysulfosuccinimide (NHS) and 1-ethyl-3-(3-dimethylaminopropyl) carbodiimide (EDC) were purchased from Sigma-Aldrich Chemical Co. (St. Louis, MO, U. S. A.). Cadmium chloride ($CdCl_2 \cdot 2.5H_2O$), 2-(*N*-morpholino)ethanesulfonic acid (MES) and *meso*-2,3-dimercaptosuccinic acid (DMSA) were purchased from Alfa Aesar China Ltd. (China). Trisodium citrate and chloroauric acid ($HAuCl_4 \cdot 3H_2O$) were purchased from Sinopharm Co., Ltd. (Shanghai, China). Tellurium rod (10 mm in diameter) was purchased from Leshan Kayada Photoelectricity Co., China. 0.1 M pH 9.0 phosphate buffer saline (PBS) as the detection solution was prepared by mixing stock solutions of NaH_2PO_4 and Na_2HPO_4 containing 0.1 M KNO_3. The washing buffer was 0.01 M pH 7.4 PBS. The blocking solution was 1 mM MCH aqueous solution. All other reagents were of analytical grade and were used as received. Ultrapure water obtained from a Millipore water purification system (≥18 MΩ, Milli-Q, Millipore) was used in all assays. The N_2-saturated solution was prepared by purging the solution with highly pure N_2 for 30 min.

The synthetic single-stranded oligonucleotides were purchased from Sangon Biological Engineering Technology & Services Co. Ltd. (Shanghai, China) and purified using high-performance liquid chromatography. Their sequences are listed below:

(a) 49-mer thiol modified MB (probe I): 5′-SH–$(CH_2)_6$–AAAAAA*GGG*TT*GGGCGGG*A***T*GGG*TT**ACCTCAGTGCTTATTCGA**AACCCA**-3′;

(b) 49-mer amine-modified stem-loop MB (probe II): 5′-NH_2–$(CH_2)_6$–AAAAAA*GGG*TT*GGGCGGG*A***T*GGG*TT**ACCTCAGTGCTTATTCGA**AACCCA**-3′;

(c) 49-mer carboxyl-modified stem-loop MB (probe III): 5′-COOH–$(CH_2)_6$–AAAAAA*GGG*TT*GGGCGGG*A***T*GGG*TT**ACCTCAGTGCTTATTCGA**AACCCA**-3′;

(d) 18-mer complementary target DNA: 5′-TCGAATAAGCACTGAGGT-3′;

(e) 18-mer partial complementary ssDNA with one-base mismatch: 5′-TCGACTAAGCACTGAGGT-3′;

(f) 18-mer partial complementary ssDNA with two-base mismatch: 5′-TCGACTACGCACTGAGGT-3′;

(g) 18-mer partial complementary ssDNA with three-base mismatch: 5′-TCGACTACGTACTGAGGT-3′.

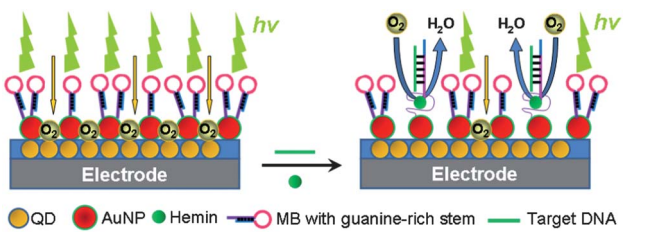

Scheme 1 Schematic illustration of QDs-based ECL DNA sensing by quenching of ECL emission upon hybridization with the molecular beacon to form hemin/G-quadruplex architecture.

Apparatus

Photoluminescence (PL) and UV-vis absorption spectra were recorded on a RF-5301 PC fluorometer (Shimadzu Co., Japan) and a Shimadzu UV-3600 UV-vis-NIR photospectrometer (Shimadzu Co., Japan), respectively. The solid-state fluorescence spectra were collected with an Edinburgh FLS920 fluorescence spectrometer (Livingston, UK). Tapping mode atomic force microscopy (AFM) images of the samples cast on freshly cleaved mica sheets were acquired under ambient conditions using an Agilent 5500 AFM/SPM system (U. S. A.) and Picoscan v5.3.3 software. Electrochemical impedance spectroscopy (EIS) measurements were carried out on a PGSTAT30/FRA2 system (Autolab, the Netherlands) in 0.1 M KNO_3 containing 5 mM $K_3Fe(CN)_6/K_4Fe(CN)_6$ with a frequency range of 10^{-1} to 10^5 Hz and an amplitude of 5 mV. Cyclic voltammetry experiments were performed on a CHI 812B electrochemical workstation (CH Instruments Inc., U. S. A.). Electrochemiluminescence (ECL) measurements were carried out on a MPI-E multifunctional electrochemical and chemiluminescent analytical system (Xi'an Remex Analytical Instrument Ltd. Co., China). A modified glassy carbon electrode (GCE, 5 mm in diameter) working electrode, a platinum wire counter electrode and a Ag/AgCl (saturated KCl) reference electrode were used in all electrochemical measurements, and all potentials were quoted against this reference electrode. The ECL cell was self-made with three side necks and one middle neck. The reference and counter electrodes were put in two side necks, while the GCE was put in the middle neck with its surface downward, approximating the optical window for recording the ECL signal. Another side neck was used for bubbling gas and injecting samples. The ECL emission window was placed in front of the photomultiplier tube (PMT, detection range from 300 to 650 nm) biased at −800 V. Unless specified, the scan rate was 100 mV s^{-1}.

Preparation of DMSA-stabilized QDs

DMSA-stabilized CdTe (DMSA–CdTe) QDs were synthesized by the electrolysis method.[16] First, 6.0 mg of DMSA was dissolved by stirring in 20 mL ultrapure water containing 200 μL 1.0 M NaOH to help the dissolution and regulate pH at around 10. Then 120 μL of 0.1 M $CdCl_2$ was added dropwise to obtain a homogeneous solution. After highly pure N_2 was bubbled through the solution for 20 min, potentiostatic voltammetry was carried out at −1.0 V in the solution, with a tellurium rod as a working electrode. The solution remained in the N_2

atmosphere during the whole process, while the applied potential was tuned promptly by monitoring the current around 0.12 mA until a terminal charge quantity of 0.5 C was reached. The resulting solution was sealed and refluxed at 80 °C for 20 h to harvest the DMSA–CdTe QDs, and stored at 4 °C prior to use. Before modification, the as-prepared QDs solution was purified and precipitated in 1 : 1 (v/v) isopropyl alcohol–water and centrifuged at 5000 RCF for 5 min. Decanting the supernatant, the precipitate was then diluted in a certain amount of water.

Preparation of AuNPs

The colloidal gold nanoparticles (AuNPs) with 13 nm diameter were prepared according to the previous protocol.[17] In brief, 100 mL of 0.01% $HAuCl_4$ aqueous solution was boiled with vigorous stirring, and 2.5 mL of 1% trisodium citrate aqueous solution was quickly added to the boiling solution. The solution turned wine red, indicating the formation of AuNPs. Followed by continued stirring and cooling, the resulting Au colloidal solution was stored in brown glass bottles at 4 °C before use.

Preparation of QDs-based ECL DNA sensor and detection procedure

Prior to modification, a GCE was polished to a mirror using 1.0 and 0.05 μm alumina slurry (Beuhler), followed by sonication in ethanol and water. After the electrode was rinsed with ultrapure water and allowed to dry in a N_2 atmosphere, 20 μL of ~100 μM DMSA–CdTe QDs was dropped onto its surface. After drying in air at room temperature, 10 μL of 0.025% chitosan solution was coated on the QD film, before further coating of the 20 μL as-prepared AuNPs solution for 4 h. After rinsing with 0.01 M pH 7.4 PBS, 20 μL of MB (0.1 μM in 0.01 M pH 7.4 PBS) was dropped onto the electrode and incubated for 60 min at 36 °C and 4 °C overnight in a 100% moisture-saturated environment. The resulting electrode surface was slowly washed with a stream of 0.01 M pH 7.4 PBS to remove unbound oligonucleotides, blocked with 20 μL of 1 mM MCH (or ethanolamine) solution for 4 h at 36 °C, and then washed with PBS again to form the QDs-based ECL DNA sensor.

To carry out the recognition and ECL measurements, the biosensor was firstly incubated with 20 μL of standard solution containing 0.1 μM hemin and the target DNA of different concentrations for 50 min at 36 °C. Finally, the ECL signal was detected in air-saturated 0.1 M pH 9.0 PBS containing 0.1 M KNO_3. The obtained DNA sensor was kept at 4 °C while not in use.

Results and discussion

Spectroscopic characterization

The UV-vis spectrum of the AuNPs stabilized by citrate anions is shown in Fig. 1. The size of the AuNPs could be estimated to be 13.1 nm from the absorption peak at 519 nm (Fig. 1, curve a),[18] which was confirmed by transmission electron microscopy (TEM) (Fig. 1, inset). CdTe QDs with *meso*-2,3-dimercapto-succinic acid (DMSA) as the capping agent (DMSA–CdTe QDs) were employed as the ECL emitters. Their UV-vis spectrum

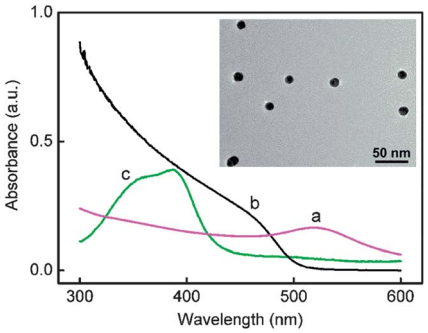

Fig. 1 UV-vis absorption spectra of AuNPs (a), DMSA–CdTe QDs (b) and hemin (c). Inset: TEM image of AuNPs.

exhibited a wide absorption band with an absorption inflection point at 466 nm (Fig. 1, curve b). According to Peng's empirical equations,[19] the size and concentration of the DMSA–CdTe QDs solution could be estimated at 0.97 nm and 10.3 μM respectively, with the band gap calculated to be 2.62 eV (1s–1s transition).[20]

Characterization of fabrication and recognition of biosensor

The three-dimensional atomic force microscopic (AFM) image of the QDs film on an indium tin oxide (ITO) slide displays densely arranged grain-like stacks of QDs, with the average height less than 4 nm (Fig. 2A). After chitosan was coated on the film, a relatively smooth morphology emerged due to the good film-forming capability of chitosan (Fig. 2B). The average height became 10 nm. After negatively-charged AuNPs were cast onto chitosan through the interactions between Au and the abundant amines of chitosan, the surface height further increased (Fig. 2C). The undulating surface profile consisting of relatively large aggregates demonstrated the successful attachment of AuNPs, which enabled the subsequent immobilization of alkylthiol-terminated nucleotides.

The stepwise fabrication and the recognition of the proposed DNA assay were further confirmed by electrochemical impedance spectra (EIS). As shown in Fig. 3, the bare glassy carbon electrode (GCE) showed a relatively small electron-transfer resistance (R_{ct}) (Fig. 3, curve a), while the R_{ct} of QDs-modified GCE was ~1800 Ω due to the intrinsic semiconductivity (Fig. 3, curve b). After covering with chitosan, the R_{ct} decreased slightly, which was ascribed to its exposed amino groups facilitating the electromigration of ferri-/ferro-cyanide and the good film-making capability uniformly redistributing the QDs (Fig. 3,

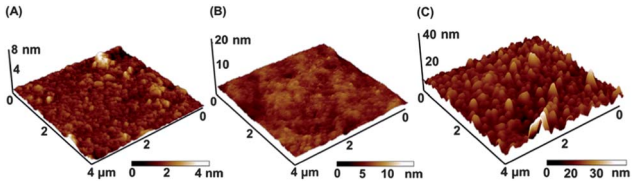

Fig. 2 AFM topographies of (A) DMSA–CdTe QDs, (B) chitosan/QDs and (C) AuNPs/chitosan/QDs modified ITO slides.

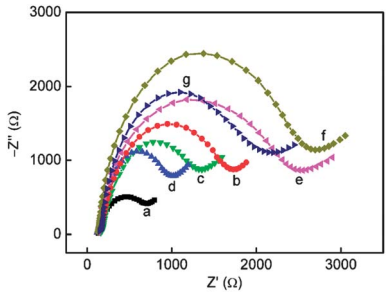

Fig. 3 EIS plots of bare GCE (a), QDs/GCE (b), chitosan/QDs/GCE (c), AuNPs/chitosan/QDs/GCE (d), MB/AuNPs/chitosan/QDs/GCE (e), MCH/MB/AuNPs/chitosan/QDs/GCE (f) and hemin + target DNA/MCH/MB/AuNPs/chitosan/QDs/GCE (g).

curve c).[21] The presence of AuNPs greatly decreased the R_{ct} (curve d), indicating that the high electrical conductivity of the AuNPs could promote charge transfer between the electrode and the redox probe. Due to the steric hindrance from the stem-loop conformation of the MB with a negatively-charged phosphate backbone and insulating linear aliphatic alkylthiols,[22] an increasing trend of R_{ct} appeared during the stepwise attachment of MB and the blocking with MCH (Fig. 3, curves e and f). After the target DNA and hemin were specifically associated with the MB, the consequent double-stranded DNA favored electron channeling,[23] thus the R_{ct} of the sensor surface decreased (Fig. 3, curve g).

ECL behaviors of QDs/hemin/G-quadruplex architecture

The chitosan/QDs/GCE showed an efficient cathodic ECL emission in air-saturated pH 9.0 PBS, peaking at −1.05 V, with the dissolved oxygen as the endogenous coreactant (Fig. 4A, curve a). The presence of AuNPs did not obviously affect the ECL intensity (Fig. 4A, curve b). After immobilizing MB on the AuNPs and then blocking the active sites with MCH, the ECL intensity decreased by a certain degree (Fig. 4A, curves c and d), which resulted from their impediment to the diffusion of the coreactant from the bulk solution to the underlying QDs.[24] On incubating the formed DNA biosensor with either the individual hemin or the target, no obvious change in ECL signal could be observed (data not shown), indicating that the short target DNA strand could not open the MB to form the hemin/G-quadruplex structure.[25] On the contrary, the ECL response dropped to its original 7.5% after simultaneous incubation with both hemin and the target DNA (Fig. 4A, curve e), which validated that the hairpin could be dissociated after the MB hybridized with the target DNA upon the assistance of hemin to form hemin/G-quadruplex architecture, and the formed architecture could quench the QDs-based ECL emission. Furthermore, the designed probe with a guanine-rich sequence in the stem-loop structure could effectively prevent the nonspecific binding of hemin to nucleic acids.

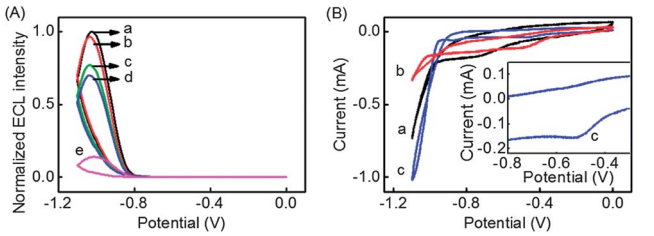

Fig. 4 (A) ECL curves of chitosan/QDs/GCE (a), AuNPs/chitosan/QDs/GCE (b), MB/AuNPs/chitosan/QDs/GCE (c), MCH/MB/AuNPs/chitosan/QDs/GCE (d), and (d) incubated with 20 μL of 1 μM hemin and 1 μM target DNA (e) in air-saturated pH 9.0 PBS. (B) Cyclic voltammograms of MCH/MB/AuNPs/chitosan/QDs/GCE before (a) and after (b) incubation with 20 μL of 1 μM hemin and 1 μM target DNA in air-saturated 0.1 M pH 9.0 PBS, and (b) in N_2-saturated 0.1 M pH 9.0 PBS (c). Inset: local magnification of (c).

The cyclic voltammetric curve of MCH/MB/AuNPs/chitosan/QDs/GCE in air-saturated pH 9.0 PBS showed one obvious reduction peak at −0.78 V (Fig. 4B, curve a), which was attributed to the electrochemical reduction of the dissolved oxygen to produce another coreactant, H_2O_2. After the MB was bound to the target DNA and hemin to form DNAzyme, the peak for oxygen reduction disappeared and a new reduction peak occurred at around −0.50 V (Fig. 4B, curve b), which was much stronger than that in N_2-saturated 0.1 M pH 9.0 PBS (Fig. 4B, curve c). The new peak could be ascribed to the direct electrochemistry of hemin(Fe^{III})/DNAzyme, and the catalytic reduction of O_2 to OH^- by DNAzyme increased the reduction peak of hemin(Fe^{III})/DNAzyme to hemin(Fe^{II})/DNAzyme. The electrode process could be described by the following mechanism:

$$\text{Hemin}(Fe^{III})/\text{DNAzyme} + e^- \rightarrow \text{Hemin}(Fe^{II})/\text{DNAzyme} \quad (1)$$

$$4\text{Hemin}(Fe^{II})/\text{DNAzyme} + O_2 + 2H_2O \rightarrow 4\text{Hemin}(Fe^{III})/\text{DNAzyme} + 4OH^- \quad (2)$$

Therefore, the dissolved oxygen as the endogenous coreactant was consumed *via* the electrocatalytic reduction by DNAzyme, which prohibited the subsequent formation of the excited state CdTe QD*, thus annihilating the ECL emission of the QDs.

Solid-state PL of G-quadruplex/hemin/QDs

In order to exclude the effect of electron transfer on the ECL emission, the solid-state PL behavior was investigated. The PL spectrum of the MCH/MB/AuNPs/chitosan/QDs modified ITO slide with an excitation wavelength (λ_{ex}) of 380 nm displayed two peaks at 464 and 588 nm (Fig. 5, curve a). The emission peak at short wavelength approximated the inflection point of UV-vis absorption, indicating the band gap emission of the core.[26] Meanwhile, the emission peak at long wavelength was attributed to the surface-states-derived emission, which is usually red-shifted by hundreds of nanometers compared to the PL emission from the core.[27] The emission peak at 588 nm suggested lower energy, *i.e.* the band gap of the surface trap was narrower than that of the core, leading to a possibility to irradiate ECL at a relatively low potential.[28] After the MB reacted with the target DNA and then bound hemin, the corresponding PL emission did not show an obvious change (Fig. 5, curve c).

As a comparison, a MCH/MB/QDs modified ITO slide was prepared by generating amido bonds between the amine-terminated probe and the carboxyl groups of DMSA. Its

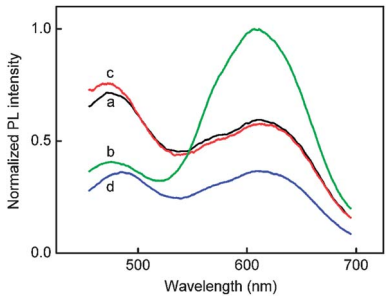

Fig. 5 Solid-state PL spectra of MCH/MB/AuNPs/chitosan/QDs (a and c) and MCH/MB/QDs (b and d) modified ITO slides before (a and b) and after (c and d) incubation with 20 μL of 1 μM hemin and 1 μM target DNA in air-saturated 0.1 M pH 9.0 PBS (λ_{ex} = 380 nm).

surface-states PL emission showed a drop of 62.2% upon the formation of hemin/G-quadruplex architecture (Fig. 5, curves b and d). The quenching process was reported *via* an electron transfer mechanism,[29,30] whereas the photoexcited electrons at the conduction band were transferred to hemin.[9,10] As the electron transfer only took place within several nanometers in the electrolyte solution, it was hard to influence the PL emission of the QDs covered with chitosan and AuNPs as spacers. Furthermore, apart from the broad Soret band at 395 nm (Fig. 1, curve c),[31] 1 μM hemin lacked any obvious absorbance in the luminescent range of the QDs, and thus annihilation through the fluorescence resonance energy transfer (FRET) route could be eliminated. In other words, the ECL quenching mechanism relied on the consumption of coreactant by hemin/G-quadruplex DNAzyme rather than electron transfer or FRET.

Optimization of detection conditions

The ECL quenching efficiency mainly depended on the amount of the formed hemin/G-quadruplex DNAzyme on the electrode, which was codetermined by the amount of immobilized MB and its hybridization with target DNA in the presence of hemin. Three methods for the immobilization of MB were examined as follows: (a) the thiol-terminated MB (MB–SH) interacted with the AuNPs through Au–S coordination; (b) the amine-modified MB (MB–NH_2) was directly covalently bonded with the *cis*-dicarboxylic ligand of the QDs through EDC and NHS coupling; (c) the carboxyl-terminated MB (MB–COOH) was crosslinked with the multiple amino groups of chitosan by EDC–NHSS reaction. Method (a) achieved the largest quenching coefficient of 92.5%, which was considered to be a result of the large surface-to-volume ratio of the AuNPs. Meanwhile, the quenching efficiency of method (b) was 71.6%, larger than the value of 59.2% for method (c), which may be attributed to the fewer linking ligands of the surface unpassivated DMSA–CdTe QDs, or the steric hindrance on the chitosan film. Furthermore, since the electron transfer normally occurred within a short range, the catalytic consumption of coreactant by hemin could dominate the ECL quenching in method (a). Therefore, method (a) was used for immobilization of MB.

The incubation time is an important parameter in a DNA assay. With increasing incubation time at 36 °C for the recognition of the MB to the target DNA and hemin, the ECL intensity quickly diminished and reached a plateau at 50 min (Fig. 6A), which was thus used for the target DNA assay. The concentration of MB used in the preparation of the biosensor also greatly affected the ECL intensity. When the concentration of MB was increased, the ECL emission dropped drastically and then remained steady at 0.1 μM, indicating a saturated immobilization of the MB on AuNPs (Fig. 6B). Thus, 0.1 μM MB was chosen. In addition, to guarantee the maximal formation of the hemin/G-quadruplex DNAzyme, the amount of hemin was also settled at 0.1 μM.

ECL DNA sensing

Taking advantage of the efficient low-potential ECL emission of DMSA–CdTe QDs, a facile "signal-off" strategy was proposed for the detection of target DNA based on the consumption of coreactant. As shown in Fig. 7, the ECL peak intensity at −1.05 V decreased with the increasing target DNA concentration. The calibration plot showed a good linear relationship between the ECL intensity and the logarithmic value of the target concentration ranging from 5.0 fM to 0.1 nM, with a correlation coefficient of 0.992 (Fig. 7, inset). The detection limit at a signal-to-noise ratio of 3 was 0.9 fM, indicating high sensitivity. More importantly, the developed DNA sensor showed a wide detection range of 5 orders of magnitude and avoided the need for the tagging and deoxygenation of general electrochemical DNA assays.

Reproducibility and stability of the DNA sensor

The DNA sensor showed good specificity for sequence detection of the target DNA. After the mixture of 0.1 μM hemin and 0.1 nM single-base, two-base or three-base mismatched DNA oligonucleotide was dropped onto the MCH/MB/AuNPs/chitosan/QDs/GCE for hybridization, the proposed biosensor showed much weaker ECL variations than that hybridized with complementary DNA at the same concentration. The corresponding quenching percentages resulting from the three sequences were 22.4%, 17.6% and 9.3% of that for the complementary target DNA, respectively (Fig. 8A). It was the thermodynamic factor that restrained the hybridization of mismatched sequence with the probe DNA.[32] Both the intra-assay and inter-assay precisions of the QDs-based ECL DNA sensor were examined for 0.1 nM target DNA five times. The relative standard deviations (RSD)

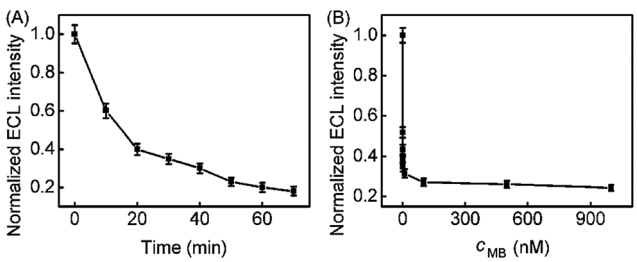

Fig. 6 Effects of (A) incubation time on the hybridization of target DNA and binding of hemin, and (B) concentration of MB for its immobilization on ECL intensity.

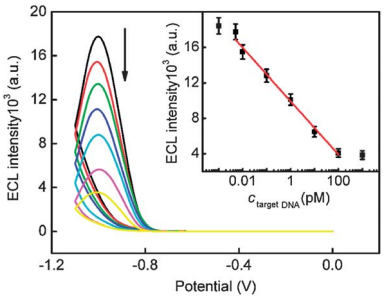

Fig. 7 ECL responses of the proposed DNA sensor to target DNA at 0, 5.0 fM, 10.0 fM, 0.1 pM, 1.0 pM, 10.0 pM, 0.1 nM and 1.0 nM (from top to bottom) in air-saturated 0.1 M pH 9.0 PBS. Inset: calibration curve ($n = 3$).

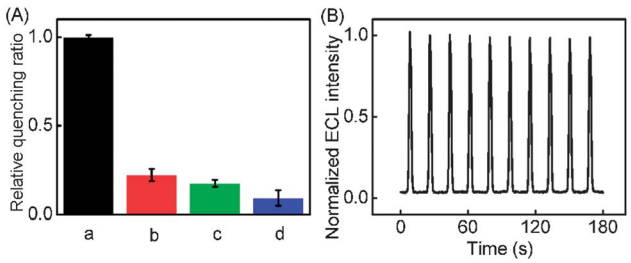

Fig. 8 (A) ECL quenching ratio of MCH/MB/AuNPs/chitosan/QDs/GCE after incubation with 20 μL of 0.1 μM hemin and 0.1 nM target DNA (a), 1-mismatch (b), 2-mismatch (c) and 3-mismatch (d) ssDNA. (B) Continuous cyclic scans of the DNA sensor in an air-saturated detection solution after incubation with 20 μL of 0.1 μM hemin and 0.1 nM target DNA.

were 2.2% and 6.1%, respectively, showing the good precision and acceptable fabrication reproducibility. Ten measurements of ECL emission upon continuous cyclic scans of the ECL immunosensor for 0.1 nM target DNA showed coincident signals with a RSD of 1.1% (Fig. 8B), indicating the good reliability and stability of the detection signal.

Conclusions

A label-free QDs-based ECL system for DNA assay has been developed based on the consumption of coreactant by the electrocatalytic reduction of dissolved oxygen by DNAzyme. The DNAzyme can be formed *in situ* on the biosensor surface by the recognition of the immobilized MB with a thiolated guanine-rich stem to the target DNA with the assistance of hemin. Due to the requirement of the coexistence of hemin and the target DNA to open up the hairpin structure of the probe to form the hemin/G-quadruplex architecture, the designed MB can effectively prevent the nonspecific binding of hemin to nucleic acids. The formed hemin/G-quadruplex architecture has been proved to have high electrocatalytic activity toward the reduction of O_2, and thus quenches the ECL emission. Based on the efficient ECL quenching, the proposed ECL biosensor exhibits high sensitivity and a wide linear range over 5 orders of magnitude, with acceptable reproducibility and stability. This work provides a new method for the formation of DNAzyme, a new application for QDs-based ECL biosensing and a power protocol for the detection of DNA.

Acknowledgements

This work was financially supported by the National Basic Research Program of China (2010CB732400), the National Natural Science Foundation of China (20835006, 21121091, 21135002), and Excellent Talents in University (NCET100479).

Notes and references

1 X. B. Yin, *TrAC, Trends Anal. Chem.*, 2012, **33**, 81.
2 S. R. Ryoo, H. Jang, K. S. Kim, B. Lee, K. B. Kim, Y. K. Kim, W. S. Yeo, Y. Lee, D. E. Kim and D. H. Min, *Biomaterials*, 2012, **33**, 2754.
3 X. Q. Liu, R. Freeman, E. Golub and I. Willner, *ACS Nano*, 2011, **5**, 7648.
4 A. Vallee-Belisle, F. Ricci and K. W. Plaxco, *J. Am. Chem. Soc.*, 2012, **134**, 2876.
5 L. H. Tang, Y. Liu, M. M. Ali, D. K. Kang, W. A. Zhao and J. H. Li, *Anal. Chem.*, 2012, **84**, 4711.
6 G. F. Jie, L. Wang, J. X. Yuan and S. S. Zhang, *Anal. Chem.*, 2011, **83**, 3873.
7 H. Zhou, J. Liu, J. J. Xu and H. Y. Chen, *Chem. Commun.*, 2011, **47**, 8358.
8 Y. Shan, J. J. Xu and H. Y. Chen, *Nanoscale*, 2011, **3**, 2916.
9 C. Teller, S. Shimron and I. Willner, *Anal. Chem.*, 2009, **81**, 9114.
10 M. Y. Zhou, Y. Liu, Y. F. Tu, G. H. Tao and J. L. Yan, *Biosens. Bioelectron.*, 2012, **35**, 489.
11 G. Pelossof, R. Tel-Vered and I. Willner, *Anal. Chem.*, 2012, **84**, 3703.
12 G. Pelossof, R. Tel-Vered, J. Elbaz and I. Willner, *Anal. Chem.*, 2010, **82**, 4396.
13 D. Li, B. Shlyahovsky, J. Elbaz and I. Willner, *J. Am. Chem. Soc.*, 2007, **129**, 5804.
14 T. Niazov, V. Pavlov, Y. Xiao, R. Gill and I. Willner, *Nano Lett.*, 2004, **4**, 1683.
15 D. J. Lin, J. Wu, F. Yan, S. Y. Deng and H. X. Ju, *Anal. Chem.*, 2011, **83**, 5214.
16 C. W. Ge, M. Xu, J. Liu, J. P. Lei and H. X. Ju, *Chem. Commun.*, 2008, 450.
17 A. Ambrosi, M. T. Castañeda, A. J. Killard, M. R. Smyth, S. Alegret and A. Merkoçi, *Anal. Chem.*, 2007, **79**, 5232.
18 S. J. Hurst, A. K. R. Lytton-Jean and C. A. Mirkin, *Anal. Chem.*, 2006, **78**, 8313.
19 W. W. Yu, L. H. Qu, W. Z. Guo and X. G. Peng, *Chem. Mater.*, 2003, **15**, 2854.
20 L. Sun, L. Bao, B. R. Hyun, A. C. Bartnik, Y. W. Zhong, J. C. Reed, D. W. Pang, H. D. Abruña, G. G. Malliaras and F. W. Wise, *Nano Lett.*, 2009, **9**, 789.
21 M. M. Ali, S. D. Aguirre, H. Lazim and Y. F. Li, *Angew. Chem., Int. Ed.*, 2011, **50**, 3751.
22 S. J. He, B. Song, D. Li, C. F. Zhu, W. P. Qi, Y. Q. Wen, L. H. Wang, S. P. Song, H. P. Fang and C. H. Fan, *Adv. Funct. Mater.*, 2010, **20**, 453.
23 C. D. S. Riccardi, C. Kranz, J. Kowalik, H. Yamanaka, B. Mizaikoff and M. Josowicz, *Anal. Chem.*, 2008, **80**, 237.

24 A. X. Zheng, J. Li, J. R. Wang, X. R. Song, G. N. Chen and H. H. Yang, *Chem. Commun.*, 2012, **48**, 3112.
25 G. Ananyan, A. Avetisyan, L. Aloyan and Y. Dalyan, *Biophys. Chem.*, 2011, **156**, 96.
26 N. Myung, Z. Ding and A. J. Bard, *Nano Lett.*, 2002, **2**, 1315.
27 Y. J. Bae, N. Myung and A. J. Bard, *Nano Lett.*, 2004, **4**, 1153.
28 G. D. Liang, L. P. Shen, G. Z. Zou and X. L. Zhang, *Chem.–Eur. J.*, 2011, **17**, 10213.
29 R. Freeman and I. Willner, *Nano Lett.*, 2009, **9**, 322.
30 X. H. Zhao, R. M. Kong, X. B. Zhang, H. M. Meng, W. N. Liu, W. H. Tan, G. L. Shen and R. Q. Yu, *Anal. Chem.*, 2011, **83**, 5062.
31 Y. X. Xu, L. Zhao, H. Bai, W. J. Hong, C. Li and G. Q. Shi, *J. Am. Chem. Soc.*, 2009, **131**, 13490.
32 G. Bonnet, S. Tyagi, A. Libchaber and F. R. Kramer, *Proc. Natl. Acad. Sci. U. S. A.*, 1999, **96**, 6171.